JOURNAL OF SOLID STATE CHEMISTRY 34, 389–396 (1980)

A Mössbauer and X-Ray Study of $Fe_2P_{1-x}B_x$ Compounds ($x < 0.15$)

R. CHANDRA*, S. BJARMAN, T. ERICSSON, L. HÄGGSTRÖM, C. WILKINSON†, AND R. WÄPPLING

Institute of Physics, University of Uppsala, Box 530, S-751 21 Uppsala, Sweden

AND Y. ANDERSSON AND S. RUNDQVIST

Institute of Chemistry, University of Uppsala, Box 531, S-751 21 Uppsala, Sweden

Received August 31, 1979; in final form November 24, 1979

Boron/phosphorus substitution in Fe_2P has been studied by ^{57}Fe Mössbauer spectroscopy. The magnetic ordering temperature increases rapidly with increasing boron content. Replacement of a phosphorus atom by boron in the immediate environment of an iron atom results in a substantial increase of the magnetic hyperfine field, while the centroid shift and the quadrupole splitting are almost unchanged. The hyperfine parameters for iron atoms at larger distances from the boron atom remain unaffected. Boron substitutes preferentially for phosphorus at the singlefold P(2) position in the Fe_2P structure.

1. Introduction

The present paper gives an account of Mössbauer spectroscopic studies of substitutional solid solutions of boron in Fe_2P, corresponding to the formula $Fe_2P_{1-x}B_x$ ($x < 0.15$). Since detailed knowledge of the crystallographic and magnetic properties of pure Fe_2P is essential to an interpretation of the Mössbauer results, a summary of available information is given below.

The crystal structure of Fe_2P (low-pressure form (*1*)) was determined by Rundqvist and Jellinek (*2*) and accurately refined by Carlsson *et al.* (*3*). The symmetry is hexagonal (space group $P\bar{6}2m$) and the unit cell contains six iron atoms situated on two threefold positions: Fe(1) and Fe(2), and three phosphorus atoms situated on one twofold: P(1), and one singlefold: P(2), position. The Fe(1) atoms have two P(1) and two P(2) near neighbors situated at the corners of a distorted tetrahedron. The Fe(2) atoms have one P(1) and four P(2) near neighbors at the corners of a distorted square pyramid (see Fig. 1). In addition, the Fe(1) atoms have eight near-iron neighbors, and the Fe(2) atoms ten near-iron neighbors.

* On leave from Department of Physics, University of Rajasthan Jaipur, 302004, India.

† On leave from Physics Department, Queen Elizabeth College London University, London, England.

0022-4596/80/120389-08$02.00/0

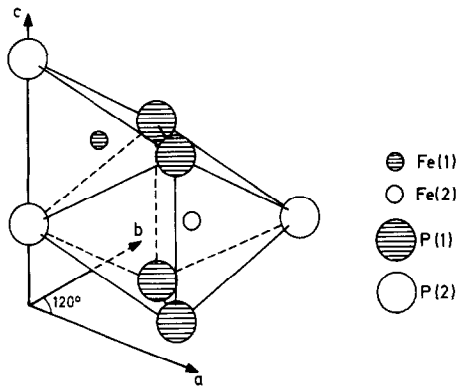

FIG. 1. The nearest phosphorus surroundings for Fe(1) and Fe(2) in Fe_2P showing the distorted tetrahedral and the distorted square-based pyramidal coordination.

The magnetic properties of Fe_2P have been the subject of numerous studies by various techniques (*4–25*). The results reported differ considerably from one another, however, and the cause of the discrepancies has remained obscure until recently. Present knowledge can be summarized as follows:

Pure Fe_2P of ideal stoichiometric composition exhibits a first-order para/ferromagnetic transition near 216 K (*18, 21, 22*). The saturation magnetic moment per formula unit amounts to approximately 2.9 μ_B (*12, 21, 22, 24*). The Curie temperature and the character of the transition are extremely sensitive to the presence of vacancies and impurity atoms in the structure, as well as to the magnitude of the external magnetic field. Since many of the earlier studies were performed on impure or insufficiently characterized samples, the results obtained were not representative for the pure Fe_2P phase. The saturation moment is less sensitive to impurities or deviations from ideal stoichiometry; nevertheless, a wide range of values has been reported. The cause of these conflicting results lies in the exceedingly large magnetic anisotropy of Fe_2P (*21, 22*), leading to a very slow approach to saturation when magnetization measurements are made on polycrystalline samples. Extrapolation to infinite fields from low-field data is accordingly a most unsatisfactory procedure for determining the saturation moment, but many of the earlier values reported were actually based on this technique.

The Mössbauer spectrum of Fe_2P in the ferromagnetic state can be decomposed into two six-line components. The assignment of these components to the two nonequivalent iron positions in the structure (*8–10, 14, 18, 19*) is in agreement with the magnetic structure as determined by neutron diffraction (*24*). The Mössbauer spectrum of paramagnetic Fe_2P can be decomposed into four absorption lines, corresponding to a quadrupole-split doublet for each of the two iron positions. Different ways of pairing the lines into doublets and assigning them to the iron positions have been proposed, but recent experiments provide an unambiguous interpretation (*20, 25, 26*).

The occurrence of P/B substitution in Fe_2P was first observed by Rundqvist (*27*), who reported a maximum substitution of the order of 10% at 1000°C. Roger (*12*) made a cursory examination of the magnetic properties of $Fe_2P_{1-x}B_x$ and found that the Curie temperature increases rapidly with increasing boron content.

Substitution of nonmetal atoms for phosphorus in Fe_2P was considered by Rundqvist (*28*) from the size-factor point of view. He proposed that nonmetal atoms having a larger radius than phosphorus (e.g., silicon and arsenic) should preferentially occupy the P(1) site, while nonmetal atoms of smaller radius (e.g., boron) should occupy the P(2) site. This idea was confirmed by X-ray diffraction measurements in the case of arsenic substitution (*16*). The present results indicate that the prediction is also correct for boron substitution.

2. Experimental Details

2.1. Synthetic Work

Master alloys of Fe_2P and Fe_2B were synthesized from iron (spectroscopically standardized iron rod, Johnson, Matthey et Co. Ltd.), red phosphorus (5N, Koch–Light Laboratories Ltd.), and boron (claimed purity 99.8%, Hermann Starck, Berlin). The iron–phosphorus alloy was prepared in exactly the same manner as described by Carlsson *et al.* (*3*). Fe_2B was obtained by arc-melting iron and boron. Three samples $Fe_2P_{1-x}B_x$ with $x = 0.04$, 0.08, and 0.15 were prepared by mixing appropriate amounts of the master alloys and heating in evacuated and sealed silica tubes at 1273 K for 3 days. The products were checked by X-ray diffraction, and the heat treatment was repeated two or three times in order to obtain equilibrium. For $Fe_2P_{0.85}B_{0.15}$, the temperature at the final heat treatment was raised to 1373 K.

X-ray powder diffraction patterns were recorded in a Hägg–Guinier type focusing camera (Philips XDC-700) using $CrK\alpha_1$ radiation and silicon ($a = 5.43054$ Å) as internal calibration standard.

The powder photographs of $Fe_2P_{0.96}B_{0.04}$ and $Fe_2P_{0.92}B_{0.08}$ showed only lines from the $Fe_2P_{1-x}B_x$ phase, while traces of ϵ(Fe–P–B) and Fe_5PB_2 in the $Fe_2P_{0.85}B_{0.15}$ alloy indicated a boron content in slight excess of the $Fe_2P_{1-x}B_x$ solubility limit (*27*).

The unit-cell dimensions (standard deviations in parentheses) are given below:

$Fe_2P_{0.96}B_{0.04}$: $a = 5.8974(2)$ Å,
$c = 3.4099(3)$ Å.

$Fe_2P_{0.92}B_{0.08}$: $a = 5.9163(2)$ Å,
$c = 3.3695(3)$ Å.

$Fe_2P_{0.85}B_{0.15}$: $a = 5.9356(3)$ Å,
$c = 3.3251(3)$ Å.

2.2 Mössbauer Spectroscopy

Each sample was crushed to a fine powder under alcohol and mixed with boron nitride. The mixture was pressed to a disk containing ~10 mg/cm^2 of natural iron. These plates were used as Mössbauer absorbers in transmission geometry. The Mössbauer equipment was of the conventional constant-acceleration type with two Co*Rh* sources permitting simultaneous calibration using a natural iron foil at room temperature as standard.

Mössbauer spectra were recorded in the temperature region from 80 K to above T_c using a flow cryostat and a vacuum furnace. The temperature was controlled to within ±0.5 K. The recorded spectra were analyzed by least-squares fitting of various sets of Lorentzian lines to the experimental points.

3. Results

The Curie temperature was found to increase rapidly with increasing boron content. Furthermore, the first-order transition in pure Fe_2P was found to be suppressed when boron was added, and a transition region of about 10 K was observed in which the paramagnetic phase and the ferromagnetic phase coexist. The Curie temperature, defined as the midpoint of the transition region, is shown in Fig. 2 as a function of the composition. As seen in Fig. 3, the spectra in the paramagnetic state for the three different compositions are rather similar. The center of gravity changes with temperature as in the case of pure Fe_2P (*18*). The spectra could be fitted with two doublets of approximately the same intensity having an individual line width (FWHM) of ~0.32 mm/sec for all compositions. The appropriate parameters are given in Table I. At 80 K all spectra have the same principal features (Fig. 4) and can be fitted with four six-line patterns, the

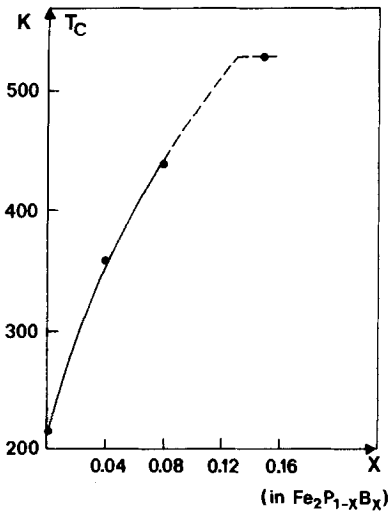

FIG. 2. Variation of Curie temperature, T_c, as a function of composition x. The ordering temperature is defined as the midpoint of the transition region of about 10 K (see text). The line drawn through the experimental points is broken in the composition range where the boron solubility limit (*27*) is exceeded.

hyperfine parameters of which being nearly unchanged at different boron contents (Table I). The relative intensities of these patterns change distinctly with composition,

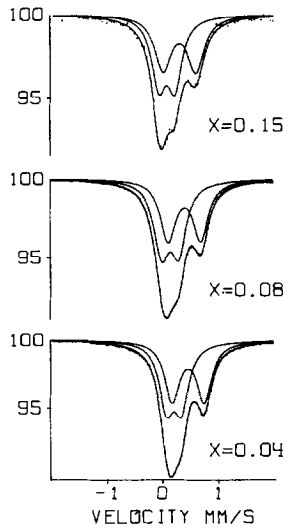

FIG. 3. Mössbauer spectra of $Fe_2P_{1-x}B_x$ with x = 0.15, 0.08, and 0.04 recorded at 543, 475, and 400 K, respectively.

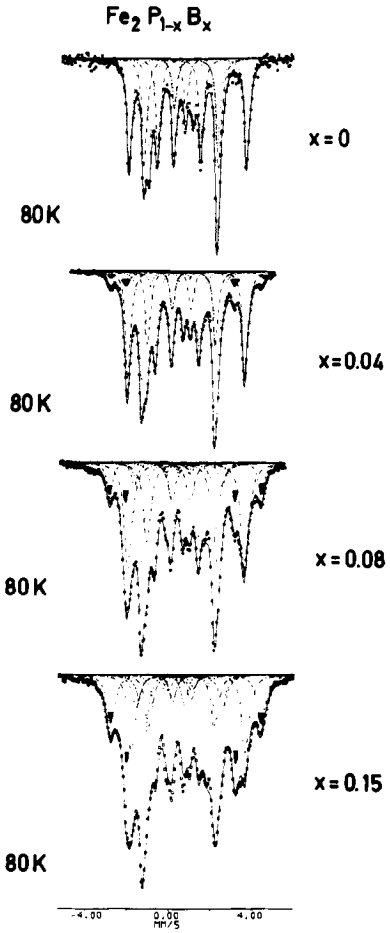

FIG. 4. Mössbauer spectra of $Fe_2P_{1-x}B_x$, with x = 0, 0.04, 0.08, and 0.15 recorded at 80 K. The outer lines of Fe(1)*b* and Fe(2)*b* are marked.

however. As the temperature increases the magnetic hyperfine fields vary differently for the different samples; cf. the room-temperature data in Table I.

4. Discussion

It is natural to interpret the two doublets in the spectra recorded above T_c as originating from the two iron positions in the crystal structure. The assignment of the doublets to Fe(1) and Fe(2) is made in accordance with the results for Fe_2P (*20, 25, 26*). The doublet with the higher centroid shift is thus assigned to Fe(2).

TABLE I

RESULTS OF THE ANALYSIS OF THE MÖSSBAUER SPECTRA

T(K)	Fe(1)a				Fe(2)a				Fe(1)b				Fe(2)b				
Sample	δ	ΔE_Q	B_{hf}	I	δ	ΔE_Q	B_{hf}	I	δ	ΔE_Q	B_{hf}	I	δ	ΔE_Q	B_{hf}	I	Γ
80 A	.41(1)	.10(1)	10.9(1)	50(1)	.66(1)	.21(1)	17.2(1)	50(1)									.28(1)
B	.41(1)	.11(1)	11.1(1)	42(3)	.66(1)	.25(1)	17.3(1)	42(3)	(.41)	(.11)	16.1(1)	10(3)	(.67)	(.25)	22.5(1)	6(2)	.31(1)
C	.42(1)	.12(1)	11.1(1)	34(2)	.67(1)	.28(1)	17.2(1)	40(3)	(.42)	(.12)	16.1(1)	15(3)	(.67)	(.28)	22.3(1)	11(2)	.42(1)
D	.42(1)	.14(2)	11.1(1)	28(2)	.68(3)	.33(4)	16.9(1)	27(3)	.40	.26(5)	16.2(1)	28(3)	(.68)	.32(5)	22.4(1)	16(2)	.43(1)
295 A	.27(1)	.26(1)	—	52(2)	.54(1)	.59(1)	—	48(2)									.40(1)
B	.27(1)	.15(1)	7.7(1)	45(3)	.53(1)	.20(2)	12.1(1)	43(2)	(.27)	(.15)	11.9(1)	8(2)	(.53)	(.20)	17.0(1)	4(2)	.40(1)
C	.30(1)	.13(1)	9.5(1)	35(1)	.52(1)	.24(1)	14.6(1)	39(1)	(.30)	(.13)	13.9(1)	15(1)	(.52)	(.24)	19.9(1)	11(1)	.37(1)
D	.30(1)	.14(2)	10.0(1)	28(2)	.53(1)	.27(4)	15.4(1)	32(3)	(.30)	.3(2)	14.6(1)	25(3)	(.53)	.2(1)	20.6(1)	15(2)	.40(1)
490 A	.15(1)	.28(1)		50(1)	.40(1)	.58(1)		50(1)									.30(1)
400 B	.20(1)	.27(1)		50(1)	.46(1)	.58(1)		50(1)									.32(1)
475 C	.14(1)	.31(1)		53(2)	.40(1)	.58(1)		47(2)									.33(1)
453 D	.08(1)	.31(1)		55(2)	.32(1)	.59(1)		45(2)									.33(1)

Note. Samples A, B, C, and D refer to Fe_2P, $Fe_2P_{0.96}B_{0.04}$, $Fe_2P_{0.92}B_{0.08}$, and $Fe_2P_{0.85}B_{0.15}$, respectively. The isomer shifts, δ, (relative to iron metal at 295 K) and the electric quadrupole splittings, ΔE_Q, are in mm/sec, and

$$\Delta E_Q = \frac{eQ\,V_{zz}}{2}\,[1 + (\eta^2/3)]^{1/2} \qquad \text{for } T > T_c,$$

$$\Delta E_Q = \frac{(v_6 - v_5) - (v_2 - v_1)}{2} \qquad \text{for } T > T_c,$$

where the symbols e, Q, V_{zz}, and η have their conventional meanings. The velocity for the ith peak is denoted v_i. I is the intensity in percent and Γ the FWHM of the individual Lorentzian lines. Integers in brackets are the estimated standard deviations referring to the last significant digit. Values for constrained parameters are placed in brackets.

As the fitted doublets have reasonably narrow lines for all compositions, we conclude that the B/P substitution has only a minor effect on the centroid shifts and the electric quadrupole interactions. Moreover, the parameters obtained are closely similar to those for pure Fe_2P as seen in Table I. In the ferromagnetic state, the spectra differ significantly from those of pure Fe_2P. Inspection of Fig. 4 immediately reveals the presence of a new component corresponding to a larger magnetic hyperfine field. The intensity of this component increases with increasing boron content. Closer analysis shows that the spectra actually have to be described in terms of four six-line components in order to obtain a reasonable fit. This result can be interpreted in analogy to the Mössbauer spectroscopic analysis of Fe_5PB_2 (*29*), the basic assumptions being as follows:

A boron atom replacing a phosphorus atom affects the hyperfine parameters only for its neighboring iron atoms, leaving more distant iron atoms virtually undisturbed. The main effect of B/P substitution is a considerable increase of the magnetic hyperfine field.

The observed four-component spectra can accordingly be interpreted in the following manner. The two components Fe(1)*a* and Fe(2)*a* (see Table I) correspond to Fe(1) and Fe(2) atoms with the same phosphorus atom near surroundings as in pure Fe_2P. The Fe(1)*b* and Fe(2)*b* components, having nearly the same isomer shifts and quadrupole splittings as Fe(1)*a* and Fe(2)*a*, respectively, but much larger magnetic hyperfine fields, correspond to Fe(1) and Fe(2) atoms with one of the near surrounding phosphorus atoms replaced by a boron atom.

For Fe_5PB_2 and Fe_5SiB_2 it was found (*29–31*) that B/P substitution did not significantly affect the centroid shift or the quadrupole splitting over the whole temperature range studied. The present results indicate that this is also true for $Fe_2P_{1-x}B_x$. To simplify the fitting procedure for the ferromagnetic spectra we therefore constrained these parameters to be the same for corresponding *a*- and *b*-type atoms.

B/P substitution can in principle occur either preferentially on P(1) or P(2) sites or randomly on both sites. Since the nonmetal atom surroundings of Fe(1) and Fe(2) are nonequivalent, the three substitution mechanisms should produce significantly different intensity distributions between the components in the Mössbauer spectra. We have accordingly calculated theoretical intensities corresponding to the three substitution mechanisms by considering the various configurational probabilities, and the results are presented in Table II. Here, Fe(1)*c* stands for an Fe(1) atom with two boron nearest neighbors, while Fe(2)*c* and Fe(2)*d* stand for Fe(2) atoms with two and three boron neighbors, respectively. In the case of completely random substitution we have assumed that the hyperfine parameters are equally affected on boron substitution for both P(1) and P(2) atoms.

Inspection of the values for the resolved Fe(1)*b* and Fe(2)*b* components in Table II clearly indicates that B/P(2) substitution is favored in $Fe_2P_{0.96}B_{0.04}$ and $Fe_2P_{0.92}B_{0.08}$. This feature agrees very well with the crystal-chemical proposal based on size-factor considerations as mentioned in the introduction.

For $Fe_2P_{0.85}B_{0.15}$ the experimental evidence is less satisfactory. In this case, additional components corresponding to iron atoms with two near boron neighbors would be expected to appear in the spectrum. The presence of Fe_5PB_2 and $Fe_3(P,B)$ in the sample adds greatly to the complexity of the analysis, however, and precludes any more definite conclusions.

The ferro to paramagnetic transition in boron-substituted Fe_2P is not of the first-order type found for pure Fe_2P (*18*). In general, the first-order transition disap-

TABLE II

CONFIGURATIONAL PROBABILITIES (IN %) TOGETHER WITH EXPERIMENTAL VALUES FOR THREE DIFFERENT BORON SUBSTITUTION MODELS

Sample	Assignment	Random	B/P(1)	B/P(2)	Experimental
$Fe_2P_{0.96}B_{0.04}$	Fe(1)*a*	85	88	77	84(6)
	Fe(2)*a*	82	78	88	84(6)
	Fe(1)*b*	14	11	21	20(6)
	Fe(2)*b*	17	20	12	12(4)
	Fe(1)*c*	1	0	1	
	Fe(2)*c*	1	2	—	
$Fe_2P_{0.92}B_{0.08}$	Fe(1)*a*	72	77	58	68(4)
	Fe(2)*a*	66	60	76	80(6)
	Fe(1)*b*	25	21	37	30(3)
	Fe(2)*b*	29	33	24	22(4)
	Fe(1)*c*	3	1	6	
	Fe(2)*c*	5	7	—	
$Fe_2P_{0.85}B_{0.15}$	Fe(1)*a*	50	60	30	56(4)
	Fe(2)*a*	42	36	55	54(6)
	Fe(1)*b*	38	35	50	56(6)
	Fe(2)*b*	40	42	45	32(4)
	Fe(1)*c*	11	5	20	
	Fe(2)*c*	15	18	—	
	Fe(2)*d*	3	4		

pears by the introduction of imperfections or impurity atoms in the Fe_2P structure, as for instance iron vacancies (*18, 22*) or Cu/Fe substitution (*19, 23, 25*). In these materials the transition regions may extend to both lower and higher temperatures compared to pure Fe_2P, and the transition regions are much wider (50–100 K). The fact that one obtains additional resolved components in the Mössbauer spectra for $Fe_2P_{1-x}B_x$ shows that the boron influence on the hyperfine fields is both more intense and more local in its character as compared to other substitutions. This behavior has also been observed in other systems with boron substitutions: Fe_3P, (*14*); Fe_5PB_2, (*29*); Fe_5SiB_2 (*30, 31*).

From the magnetic hyperfine field values and the magnetic moments given by Scheerlink and Legrand (*24*) one obtains the hyperfine field to magnetic moment ratios of 15.8 and 7.4 T/μ_B for Fe(1) and Fe(2), respectively, in pure Fe_2P at 80 K. The difference between these values is surprisingly large. Assuming that the same conversion factors apply for Fe(1)b and Fe(2)b, respectively, in the boron substituted compounds one gets 3.00, 3.19, 3.27, and 3.41 μ_B per formula units in Fe_2P, $Fe_2P_{0.96}B_{0.04}$, $Fe_2P_{0.92}B_{0.08}$, and $Fe_2P_{0.85}B_{0.15}$. Normalizing the magnetic moments to the Fe_2P value, one obtains the ratios 1 : 1.06 : 1.09 : 1.14, while the assumption of a constant hyperfine field to magnetic moment ratio for all iron positions, results in ratios of 1 : 1.07 : 1.10 : 1.15.

Magnetization measurements by Lundgren (*32*) gave 2.94, 3.04, and 3.14 μ_B/formula unit for Fe_2P, $Fe_2P_{0.96}B_{0.04}$, and $Fe_2P_{0.92}B_{0.08}$, respectively. Their magnetic

moment ratios are then 1 : 1.03 : 1.07 in reasonable agreement with the Mössbauer results.

Acknowledgments

The authors are very grateful to Dr. Leif Lundgren, Institute of Technology, Uppsala, for making available his results on magnetic moment measurements prior to publication, and to Mr. Weine Karner, Institute of Physics, Uppsala, for drawing Fig. 1. The work has been financially supported by the Swedish Natural Science Research Council.

References

1. J. P. SÉNATEUR, A. ROUAULT, P. L'HÉRITIER, R. FRUCHART, B. DEYRIS, J. ROY-MONTREUIL, AND A. MICHEL, *in* "V International Conference on Solid Compounds of Transition Elements, Uppsala (1976)," Extended Abstracts p. 43.
2. S. RUNDQVIST AND F. JELLINEK, *Acta Chem. Scand.* **13**, 425 (1959).
3. B. CARLSSON, M. GÖLIN, AND S. RUNDQVIST, *J. Solid State Chem.* **8**, 57 (1973).
4. S. CHIBA, *J. Phys. Soc. Japan* **15**, 581 (1960).
5. M.-C. CADEVILLE AND A. J. P. MEYER, *C. R. Acad. Sci.* **252**, 1124 (1961).
6. A. J. P. MEYER AND M.-C. CADEVILLE, *J. Phys. Soc. Japan, Suppl. B-1* **17**, 223 (1962).
7. M.-C. CADEVILLE, Thesis, University of Strasbourg (1965).
8. A. GÉRARD, *Bull. Soc. Belge Phys.* **1**, 43 (1966).
9. R. E. BAILEY AND J. F. DUNCAN, *Inorg. Chem.* **6**, 1444 (1967).
10. K. SATO, K. ADACHI, AND E. ANDO, *J. Phys. Soc. Japan* **26**, 855 (1969).
11. R. FRUCHART, A. ROGER, AND J. P. SÉNATEUR, *J. Appl. Phys.* **40**, 1250 (1969).
12. A. ROGER, Thesis, University of Paris (1970).
13. D. BELLAVANCE, J. MIKKELSEN, AND A. WOLD, *J. Solid State Chem.* **2**, 285 (1970).
14. R. WÄPPLING, L. HÄGGSTRÖM, S. RUNDQVIST, AND E. KARLSSON, *J. Solid State Chem.* **3**, 276 (1971).
15. E. KOSTER AND B. G. TURRELL, *Canad. J. Phys.* **51**, 830 (1973).
16. A. CATALANO, R. J. ARNOTT, AND A. WOLD, *J. Solid State Chem.* **7**, 262 (1973).
17. A. GÉRARD, F. GRANDJEAN, AND M. WAUTELET, *in* "IV International Conference on Solid Compounds of Transition Elements, Geneva (1973)," Extended Abstracts, p. 70.
18. R. WÄPPLING, L. HÄGGSTRÖM, T. ERICSSON, S. DEVANARAYANAN, B. CARLSSON, AND S. RUNDQVIST, *J. Solid State Chem.* **13**, 258 (1975).
19. M. WAUTELET, A. GÉRARD, F. GRANDJEAN, K. DE STROOPER, AND G. ROBBRECHT, *Phys. Status Solidi A* **39**, 425 (1977).
20. M. WAUTELET, A. GÉRARD, AND F. GRANDJEAN, *J. Phys.* **38**, 29 (1977).
21. H. FUJII, T. HOKABE, T. KAMIGAICHI, AND T. OKAMOTO, *J. Phys. Soc. Japan* **43**, 41 (1977).
22. L. LUNDGREN, G. TARMOHAMMED, O. BECKMAN, B. CARLSSON AND S. RUNDQVIST, *Phys. Scr.* **17**, 39 (1978).
23. Y. ANDERSSON, S. RUNDQVIST, O. BECKMAN, L. LUNDGREN AND P. NORDBLAD, *Phys. Status Solidi A* **49**, K153 (1978).
24. D. SCHEERLINK AND E. LEGRAND, *Solid State Comm.* **25**, 181 (1978).
25. T. ERICSSON, L. HÄGGSTRÖM, R. WÄPPLING, AND T. METHASIRI, *Phys. Scr.*, in press.
26. J. P. SÉNATEUR, R. MADAR, D. FRUCHART, R. FRUCHART, AND P. AURIC, *in* "VI International Conference on Solid Compounds of Transition Elements, Stuttgart (1979)," Extended Abstracts p. 188.
27. S. RUNDQVIST, *Acta Chem. Scand.* **16**, 1 (1962).
28. S. RUNDQVIST, *Ark. Kemi* **20**, 67 (1962).
29. L. HÄGGSTRÖM, R. WÄPPLING, T. ERICSSON, Y. ANDERSSON, AND S. RUNDQVIST, *J. Solid State Chem.* **13**, 84 (1975).
30. R. WÄPPLING, T. ERICSSON, L. HÄGGSTRÖM, AND Y. ANDERSSON, *J. Phys. (Paris) Colloq.* **37**, C6-591 (1976).
31. T. ERICSSON, L. HÄGGSTRÖM, AND R. WÄPPLING, *Phys. Scr.* **17**, 83 (1978).
32. L. LUNDGREN, Institute of Technology, Uppsala University, Uppsala, Sweden (private communication).